The 4th International Symposium on More Electric Aircraft Technology (MEA 2017)

8–9 November 2017

Permanent magnet synchronous machine starter/generators based high-voltage DC parallel electric power system for the more electric aircraft

Feipeng Liu[1], Lie Xu[1], Yongdong Li[1], Yuanli Kang[2], Zhiyong Wu[2]

[1]*State Key Lab of Power System, Department of Electrical Engineering, Tsinghua University, Beijing, People's Republic of China*
[2]*Beijing Aeronautical Science & Technology Research Institute, Beijing, People's Republic of China*
E-mail: lfp16@mails.tsinghua.edu.cn

Published in *The Journal of Engineering*; Received on 10th January 2018; Accepted on 17th January 2018

Abstract: A high-voltage direct current (HVDC) electric power system (EPS) has become an attractive power distribution architecture for the more electric aircraft. The structure of a typical HVDC parallel EPS based on the permanent magnet synchronous machine (PMSM) starter/generators (S/Gs) is proposed in this study. On the basis of this structure, the control strategy for a single PMSM S/G system is presented, which is suitable for wide-speed operation and high-power application. It can not only achieve both starter and generator functions but also achieve the stability of DC bus voltage. A master–slave current sharing method is derived and can be applied in the HVDC parallel system, compared with the droop-control strategy. The validity of the proposed strategies is verified by simulation studies in a Matlab/Simulation environment.

1 Introduction

Nowadays, green transportation has received widespread attention because global warming is becoming more serious, which is a common challenge for humanity. More electric aircraft (MEA) is an effective solution to the environmental pressure from the perspective of civil aviation because it replaces the traditional pneumatic power, hydraulic power and mechanical power with the electrical power, which is cleaner and more reliable [1]. The starter/generator (S/G) system, which can reduce the volume and weight of mechanical devices, is one of the most important parts of MEA technology [2].

Due to the growing capacity of the electric power system (EPS), which increases from <100 kW in the 1950 s to more than 1 MW currently, a new architecture is desired to satisfy the increasing power demand. A variable-speed variable-frequency (VSVF) system has been widely applied in the MEA, and it can combine with the wound-field synchronous S/G system, which is a typical, popular and mature S/G technology and has been implemented in B787 and A380 [3]. A typical VSVF alternating current (AC) distribution system based on the synchronous S/G is shown in Fig. 1. The voltage of a three-phase VSVF AC bus can be regulated with variable speed by adjusting the excitation current of the rotor's field winding. Also, the 230 V AC power can be transferred to ±270 V direct current (DC) power and 115 V AC power by using an auto transformer rectifier unit and transformer rectifier unit, respectively. A transformer rectifier unit is used to generate the basic 28 V DC power for the MEA.

However, there are so many disadvantages of the VSVF AC system based on the wound-field synchronous S/G system. First of all, the VSVF system is an AC EPS and it is hard to achieve parallel connection among different sources due to the differences in frequency and phase angle. In other words, it will be difficult to realise uninterrupted power supply if one generator fails [4]. What's more, the transformer's weight and volume are so large and it will be contrary to the MEA's design principles, which has a strict requirement for the power density. In addition, the application of the transformer makes it harder to achieve the bi-direction flowing ability of energy. On the other hand, the most obvious shortcoming of the wound-field synchronous S/G is the complexity of the exciting process. The rotating diode bridge structure also limits the speed range of the generator shaft. As a result, a precise and heavy gearbox is required to control the S/G's speed.

A high-voltage DC (HVDC) system is becoming more and more attractive because of its less weight, high efficiency, less energy loss and low power consumption. The most important advantage of the HVDC system is that it can achieve uninterrupted power supply with the parallel connection of different sources. Several HVDC generators are connected to enlarge the capacity of the EPS, and when a fault occurs in one of the generators, the failed generator will disconnect from the HVDC bus and the others will operate in normal mode [5]. So it is necessary to develop a high power density S/G system with HVDC power distribution. The most promising machine is the permanent magnet synchronous machine (PMSM) due to its high power density, high speed operation, high power, high voltage, and simplicity [6, 7].

In this study, the control strategy for a single S/G system based on PMSM is proposed, which is based on field-oriented control (FOC). Considering the parallel structure of the EPS, droop control has been applied in the parallel structure to achieve current sharing, but it will result in high-voltage regulation, which is not desirable for the stability of the system. A novel and simple current sharing method, which is called master–slave control, is proposed and discussed in this study, which can achieve the stability of the DC bus [8].

This paper is organised as follows. Section 2 introduces the structure of a HVDC parallel EPS and its typical loads. A single S/G system based on PMSM is also discussed in Section 2. Section 3 proposes the control strategy of the S/G system based on PMSM in detail. Vector control is applied to control PMSM and two different current sharing methods are proposed as well. Section 4 presents

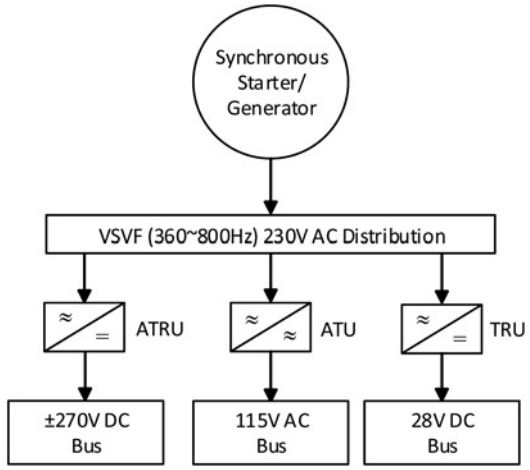

Fig. 1 *AC distribution system based on the synchronous S/G*

the simulation results to verify the theoretical analysis and a conclusion is given in Section 5.

2 System configuration

2.1 Structure of HVDC parallel EPS

The structure of the introduced HVDC parallel EPS based on PMSM S/Gs is shown in Fig. 2. In the proposed system, high-speed S/Gs are attached to the ±270 V HVDC bus through the active rectifiers, which can convert AC power to DC power, and the outputs can be connected in parallel, which is one of the most important characteristics of the HVDC system.

In starter mode, an external power will supply energy to the HVDC bus and at the same time, PMSM operates as a motor to drive the turbine to its fire speed. Once the speed reaches a specified value, PMSM will operate in generator mode. To satisfy the traditional loads of the aircraft, the inverters are required to convert HVDC to 230 and 115 V AC, which can supply power to the electrical environmental control systems, the wing ice protection system and so on. The basic 28 V DC power can be obtained through a DC/DC converter from the DC bus.

2.2 Structure of a single S/G system based on PMSM

The structure of a single S/G system based on PMSM is shown in Fig. 3. A surface PMSM is applied as the main machine of the single S/G system as a result of the trade-off studies considering mechanical and thermal constraints at high speed, reliability, and

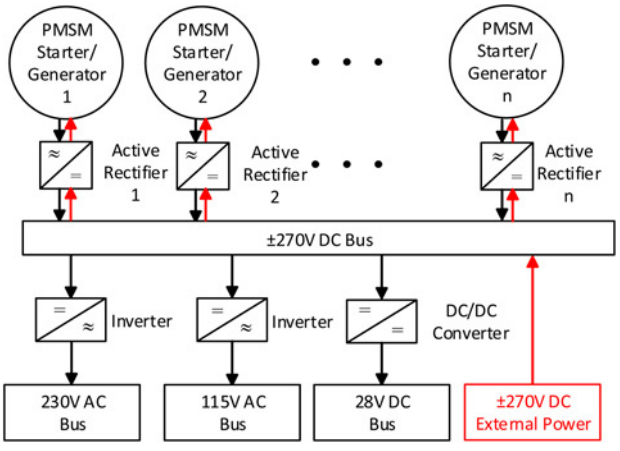

Fig. 2 *Structure of HVDC parallel EPS based on PMSM S/Gs*

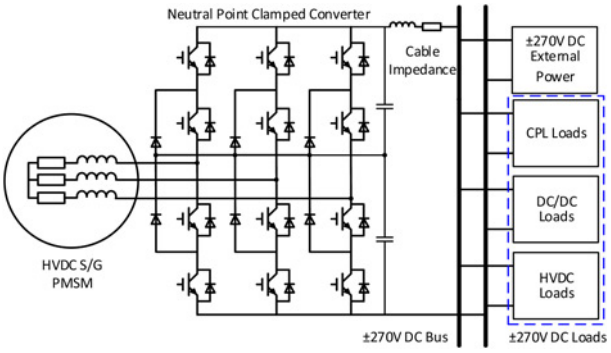

Fig. 3 *Structure of a single S/G system based on PMSM*

power density. As for the active rectifier, a three-level neutral point clamped (NPC) topology is used as a converter for the S/G system based on PMSM, which has more advantages than a traditional two-level converter, such as lower harmonic current, lower dv/dt, lower losses, etc. The cable impedance cannot be ignored in the theoretical analysis because it is larger than that in the conventional microgrids, and according to the property of loads, it can be divided into three parts, the constant power loads (CPLs), DC/DC loads and traditional HVDC loads.

3 Control scheme

3.1 Models of starter/generator system

(i) *Model of PMSM*: The model of PMSM can be described as (1)–(4), which is in the synchronously rotating dq reference frame, where the d-axis is aligned to the machine rotor

$$u_d = Ri_d + L_d \frac{\mathrm{d}i_d}{\mathrm{d}t} - \omega_e L_q i_q, \tag{1}$$

$$u_q = Ri_q + L_q \frac{\mathrm{d}i_q}{\mathrm{d}t} + \omega_e L_d i_d + \omega_e \psi_f, \tag{2}$$

$$\psi_d = L_d i_d + \psi_f, \tag{3}$$

$$\psi_q = L_q i_q, \tag{4}$$

where u_d, u_q, i_d and i_q represent the d-axis and q-axis voltage components and current components, respectively, and R, L_d and L_q are the stator resistance, d-axis, and q-axis inductances separately. ψ_d and ψ_q represent the d-axis and q-axis flux components, respectively, and ψ_f is the permanent magnet flux. ω_e is the electrical rotor speed. Also, the mechanical equations are given as

$$T_e = \frac{3}{2} p(\psi_d i_q - \psi_q i_d) = \frac{3}{2} p \psi_f i_q, \tag{5}$$

$$T_e - T_l = J \frac{\mathrm{d}\omega_r}{\mathrm{d}t} + B\omega_r, \tag{6}$$

where T_e and T_l are the electrical torque and load torque, respectively. ω_r is the mechanical rotor speed. J represents the system inertia and B is the friction coefficient. p is the pole pairs of PMSM.

(ii) Model of HVDC bus: The transient model of the HVDC bus can be written as

$$C \frac{\mathrm{d}u_{dc}}{\mathrm{d}t} = i_{dc} - i_L, \tag{7}$$

where C is the DC bus capacitor and i_{dc} is the output DC current. u_{dc} is the DC bus if the impedance of the DC cable between the NPC converter and the HVDC bus is ignored. Also, i_L is the load current. i_{dc} can be calculated through power conservation law by

(8). This model will be useful when the generator mode is analysed

$$i_{\mathrm{dc}} = \frac{P}{u_{\mathrm{dc}}} = \frac{3}{2u_{\mathrm{dc}}}(u_d i_d + u_q i_q). \tag{8}$$

(iii) Model of HVDC loads: The HVDC system's loads consist of a resistive load and CPLs, which are common and typical loads in MEA, and the model of loads can be described as (9), where P_{L} and P_{CPL} represent the total power and constant power, respectively. R is the traditional HVDC resistance

$$P_{\mathrm{L}} = \frac{u_{\mathrm{dc}}^2}{R} + P_{\mathrm{CPL}}. \tag{9}$$

3.2 Control strategy of the starter/generator system

This section will focus on the control strategy of the S/G system. Vector control is applied in the whole control scheme. FOC is the core control strategy for PMSM. According to (1)–(4), the inner current controller can be described by (10)

$$\begin{cases} u_d^* = (i_d^* - i_d)G_i - \omega_{\mathrm{e}} L_s i_q, \\ u_q^* = \left(i_q^* - i_q\right)G_i + \omega_{\mathrm{e}}(L_s i_d + \psi_f), \end{cases} \tag{10}$$

where u_d^* and u_q^* are the outputs of current controller, and i_d^*, i_q^* are the reference d-axis and q-axis currents, respectively. G_i represents the proportional-integral (PI) controller of the current loops. Fig. 4 illustrates a typical torque-speed characteristic of the PMSM used in the S/G system, where ω_{t}, ω_{p}, ω_{min} and ω_{max} represent the maximum speed of constant torque area, the maximum speed of constant power area, the minimum speed of the generator mode and the maximum speed of the generator mode.

(i) Control of starter mode: According to Fig. 4, the starter mode can be divided into two processes. The first process is constant torque control (CTC), and constant power control (CPC) is required to reduce the losses. Fig. 5 shows the control scheme of the starter mode.

To accelerate the turbine to its fire speed, a maximum torque is required to overcome the resistance. Also, the q-axis reference current can be calculated by (11) when the speed is less than ω_t and (12) is used when the process is in the constant power area

$$i_q^* = \frac{2}{3}\frac{T_{\mathrm{ref}}}{p\psi_{\mathrm{f}}}, \tag{11}$$

$$i_q^* = \frac{2}{3}\frac{T_{\mathrm{ref}}}{p\psi_{\mathrm{f}}} = \frac{2}{3}\frac{P_{\mathrm{ref}}}{p\omega_{\mathrm{r}}\psi_{\mathrm{f}}}, \tag{12}$$

where T_{ref} is the constant torque of the CTC area and P_{ref} is the constant power of the CPC area. The value of d-axis reference current is

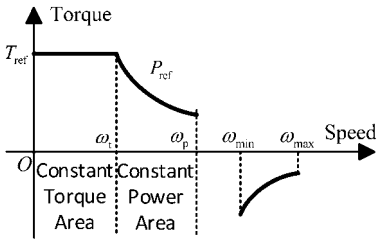

Fig. 4 *Torque-speed characteristic of the PMSM*

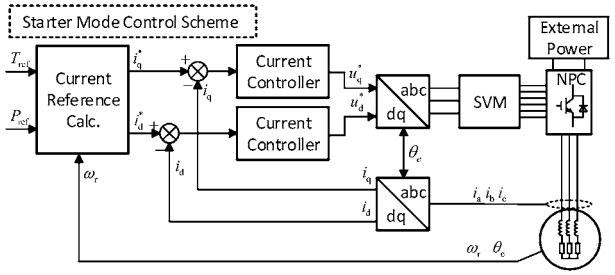

Fig. 5 *Control scheme of starter mode*

controlled to zero according to the maximum torque per ampere (MTPA) strategy, which can reduce the loss of the whole process.
(ii) Control of generator mode: The control scheme of the generator mode is illustrated in Fig. 6. The inner current loop is the same as the starter mode and the current reference controller is applied to calculate the q-axis reference current. The d-axis reference current will be calculated by the flux-weakening controller as shown in Fig. 6.

The current reference controller is the power control in essence, which means that the outer-loop controlled value can be either DC current or DC voltage. The reference value can be obtained by using the following equations:

$$i_{\mathrm{q}}^* = -(U_{\mathrm{dc}}^* - U_{\mathrm{dc}})G_u, \tag{13}$$

$$i_{\mathrm{q}}^* = -(i_{\mathrm{dc}}^* - i_{\mathrm{dc}})G_u, \tag{14}$$

Due to the limitation of the current magnitude, which can be described by (15) and the limitation of output voltage magnitude, which can be described by (16), a flux-weakening control is desired along with the increasing speed [9]

$$\sqrt{i_d^2 + i_q^2} \le i_{\mathrm{max}}, \tag{15}$$

$$\sqrt{u_d^2 + u_q^2} = \sqrt{(\omega_{\mathrm{e}} L i_q)^2 + \omega_{\mathrm{e}}^2 (L_{\mathrm{s}} i_{\mathrm{d}} + \psi_{\mathrm{f}})^2} \le u_{\mathrm{max}}, \tag{16}$$

where i_{max} and u_{max} represent the maximum value of current vector and voltage vector, respectively. The d-axis reference current can be calculated by (17), where G_{fw} represents the PI controller of the flux-weakening loop.

$$i_d^2 = \left(u_{\mathrm{max}} - \sqrt{u_d^2 + u_q^2}\right)G_{fw} \tag{17}$$

3.3 Current sharing methods

Two different methods have been proposed to achieve the current sharing between different generators. A traditional droop-control current sharing control strategy is applied in HVDC parallel EPS firstly, and a novel master–slave control method is proposed to achieve the accurate current sharing.

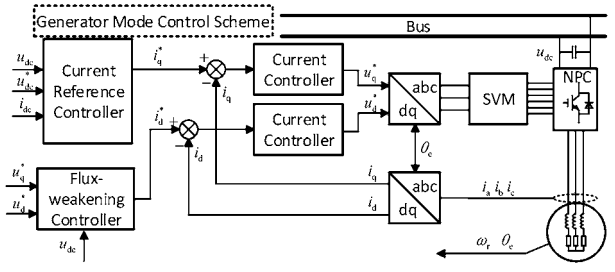

Fig. 6 *Control scheme of generator mode*

doi: 10.1049/joe.2018.0015

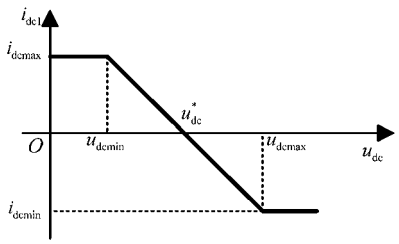

Fig. 7 *Droop-control current sharing control scheme*

(i) Droop-control current sharing method: Droop-control method is a common strategy for a parallel connection DC network and it can be applied to the HVDC parallel EPS system. It is assumed that all generators have the same power level and the droop characteristic for each generator is shown in Fig. 7. Since the DC bus voltage is the variant input and the DC current of each generator is the output, the droop-control current sharing method is called *I–V* droop [10].

Also, the reference DC current can write as (18). i_{dcref} depends on the DC bus voltage and the q-axis reference current can be calculated by using (14)

$$i_{dcref} = \begin{cases} i_{dcmax} & u_{dc} < u_{dcmin}, \\ (u^*_{dc} - u_{dc})/k & u_{dcmin} < u_{dc} < u_{dcmax}, \\ i_{dcmin} & u_{dc} > u_{dcmax}, \end{cases} \quad (18)$$

where k is the droop coefficient. The nominal voltage, u^*_{dc}, of the DC bus is 540 V in this study. The droop-control method can achieve the current sharing accurately but the result is high-voltage regulation, which will have a negative influence on the stability of the HVDC system.

(ii) Master–slave current sharing method: In this approach, a generator is selected to be the master generator, whose output current is measured by current sensors. The master–slave current sharing method is applied to select the reference current of the slave generators. In other words, the master generator is controlled by the voltage source and the others are controlled by current sources. The master–slave current sharing control scheme is shown in Fig. 8.

The main purpose of the master generator is to maintain the DC bus voltage stability. The other generators are designed to supply equal power. Assuming that the generators' capacities are equivalent, the reference current can be calculated by (19), where i_1 represent the master generator's output current

$$i_{refn} = i_1, \quad n = 2, 3, \ldots \quad (19)$$

The master–slave method can maintain the stability of DC bus voltage, but the control scheme depends on the reliability of the master generator greatly. The system will crash if the master generator fails. In this study, communication among the parallel generators is required to solve this problem.

4 Simulation studies

It is assumed that the two generators have the same power ratings and the simulation parameters are listed in Appendix A. To consider the worst case, only CPLs are taken into account in the simulation. The simulation verifications are as follows.

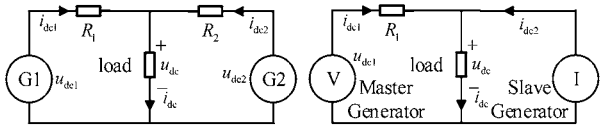

Fig. 8 *Master–slave current sharing control scheme*

4.1 Basic control verification

Fig. 9 shows the results of torque-speed characteristic in starter mode. When the speed is <7000 rpm, the output torque is about 200 Nm to accelerate the turbine, which is a constant. After the constant torque area, the PMSM is required to output constant power, causing the output torque to decrease continuously with the increase of speed. Fig. 10 presents the results of d-axis and q-axis currents. The results show that id is controlled to zero due to the MTPA control strategy and the output torque is proportional to the q-axis current according to (5). The maximum current of q-axis is about 820 A, which is corresponding to the maximum torque.

Fig. 11 shows the results of torque speed characteristic in generator mode. The speed of PMSM is shown as Fig. 11 and the load power increases or decreases by 50 kW/0.5 s. As a result, the torque varies with the change of power and speed. Fig. 12 shows the results of d-axis and q-axis current in generator mode. The flux weakening control strategy is applied when the speed

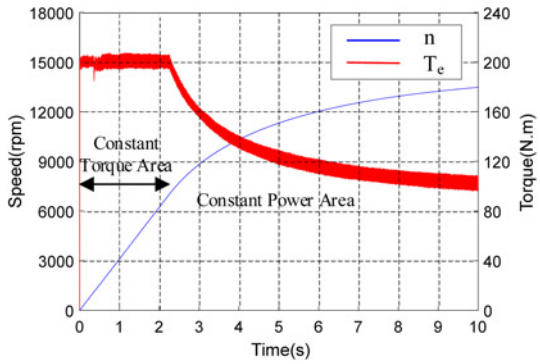

Fig. 9 *Torque-speed characteristic in starter mode*

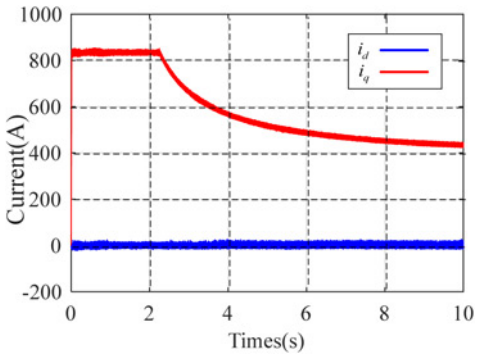

Fig. 10 *d-axis and q-axis currents in starter mode*

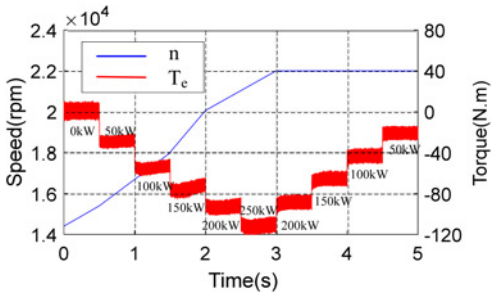

Fig. 11 *Torque-speed characteristic in generator mode*

doi: 10.1049/joe.2018.0015

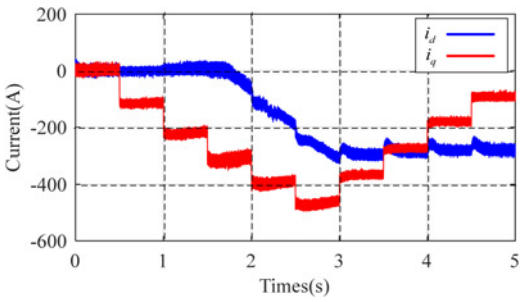

Fig. 12 *d-axis and q-axis currents in generator mode*

exceeds the turning speed, and the q-axis is corresponding to the output torque according to Figs. 11 and 12.

4.2 Current sharing control verification

The droop-control current sharing method is verified and the results are shown as Fig. 13. The DC bus voltage is 540 V when the load power is zero and it decreases along with the increasing power. When the load is 250 kW, the DC bus voltage is about 520 V. The bus voltage changes along with the load power. The output current is evenly distributed between two generators. In conclusion,

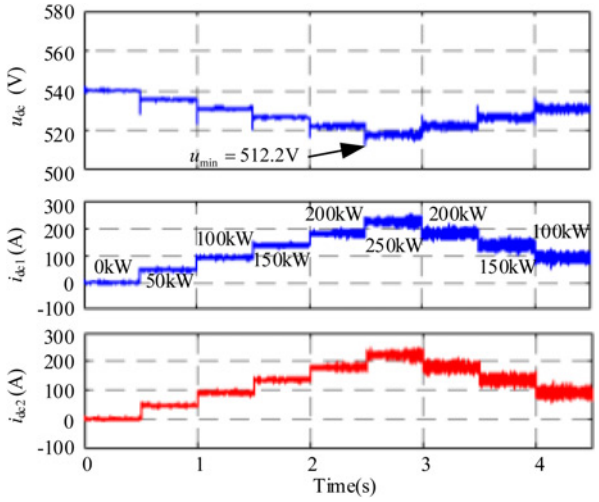

Fig. 13 *Results of droop-control current sharing control*

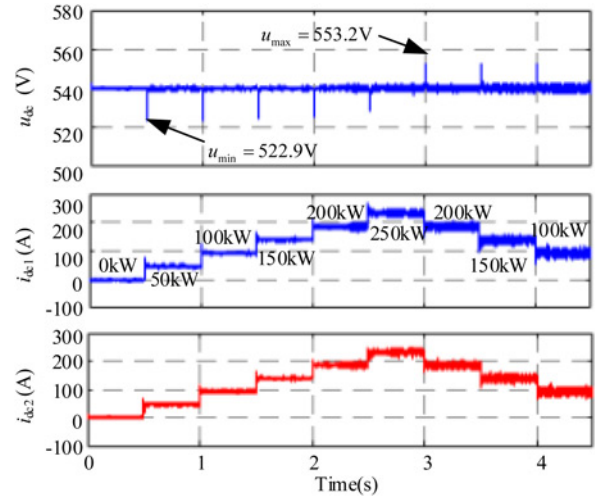

Fig. 14 *Results of master–slave current sharing control*

the droop-control method has a high voltage regulation, which will influence the stability of the whole system at some times. However, it can achieve the equal division of the current.

Fig. 14 shows the results of the master–slave current sharing method. Corresponding to the previous power and speed, the DC bus voltage can be controlled to the nominal voltage, 540 V in this study. Also, at the transient point, the maximum value of the DC bus voltage is about 553.2 V. The minimum transient voltage is about 522.9 V, but it will return to normal voltage quickly. The generator #1 shares half of the total DC current and the current sharing method is valid at different speed and different power levels.

5 Conclusion

The study has reported the detailed analysis and control design for PMSM S/G-based HVDC parallel EPS for the MEA. The structure of a HVDC parallel EPS is presented first and the S/G system based on the NPC converter is analysed. Theoretical analysis is based on the model of the S/G system and a basic control strategy is proposed in this study. A master–slave current sharing method is proposed for the HVDC parallel power system, which can realize the stability of HVDC voltage and the accurate current distribution of series generators. Another current sharing method, which is based on droop control, is compared with the 'master–slave' method. The control strategy of the S/G system and current sharing methods are successfully verified by simulation investigation.

6 References

[1] Roboam X., Sareni B., De Andrade A.: 'More electricity in the Air', *IEEE Ind. Electron. Mag.*, 2012, **6**, (4), pp. 6–17

[2] Rosero J.A., Ortega J.A., Aldabas E., *ET AL.*: 'Moving towards a more electric aircraft', *IEEE Aerosp. Electron. Syst. Mag.*, 2007, **22**, (3), pp. 3–9

[3] Li Y.N., Zhou B., Wei J.D., *ET AL.*: 'Modeling of starter/generator based on three-stage brushless synchronous machines'. Proc. Int. Conf. on Electrical and Control Engineering (ICECE 2010), 2010, pp. 5345–5348

[4] Xu Q., Chen J., Wang P., *ET AL.*: 'Investigation of the future MEA power system architecture – from the perspective of system stability'. 8th IET International Conference on Power Electronics, Machines and Drives (PEMD 2016), Glasgow, 2016, pp. 1–6

[5] Xu Y., Member S., Zhang Z., *ET AL.*: 'Current sharing in the high voltage DC parallel electric power system for the more electric aircraft'. 2016 International Conference on Electrical Systems for Aircraft, Railway, Ship Propulsion and Road Vehicles & International Transportation Electrification Conference (ESARS-ITEC), Toulouse, 2016, pp. 1–6

[6] Bozhko S., Yeoh S.S., Gao F., *ET AL.*: 'Aircraft starter-generator system based on permanent-magnet machine fed by active front-end rectifier'. 40th Annual Conf. IEEE Industrial Electronics Society (IECON 2014), 2014, pp. 2958–2964

[7] Miao D., Mollet Y., Gyselinck J., *ET AL.*: 'DC voltage control of a wide-speed-range permanent-magnet synchronous generator system for more electric aircraft applications'. 2016 IEEE Vehicle Power and Propulsion Conference (VPPC), Hangzhou, No. NSFC 51377140, 2016

[8] Gao F., Yeoh S., Bozhko S., *ET AL.*: 'Coordinated control of a DC electrical power system in the more electric aircraft integrated with energy storage'. 2015 IEEE Energy Conversion Congress and Exposition (ECCE), Montreal, QC, 2015, pp. 5431–5438

[9] Hill C., Bozhko S., Rashed M., *ET AL.*: 'Flux weakening control of permanent magnet machine based aircraft electric starter-generator'. 8th IET Int. Conf. on Power Electronics, Machines and Drives (PEMD 2016), 2016, pp. 6–6

[10] Gao F., Gu Y., Bozhko S., *ET AL.*: 'Analysis of droop control methods in DC microgrid'. 16th European Conf. on Power Electronics and Applications (EPE'14 ECCE Europe), 2014, pp. 1–9

7 Appendix I

Simulation parameters:

$u_{dc} = 540$ V, $i_{dcmax} = 500$A, $i_{dcmin} = -500$A, $u_{dcmax} = 580$ V, $u_{dcmin} = 500$ V, $k = 0.08$.